

The GRAND@Auger Prototype for the Giant Radio Array for Neutrino Detection

Beatriz de Errico,^a João R. T. de Mello Neto^{a,*} and Charles Timmermans^{b,c} for the GRAND Collaboration

(a complete list of authors can be found at the end of the proceedings)

^a*Instituto de Física, Universidade Federal do Rio de Janeiro - UFRJ ,
Ilha do Fundão , Rio de Janeiro , Brazil*

^b*Institute for Mathematics, Astrophysics and Particle Physics, Radboud Universiteit, Nijmegen, the Netherlands*

^c*Nikhef, National Institute for Subatomic Physics, Amsterdam, the Netherlands*
E-mail: beatrizspe@pos.if.ufrj.br, jtmn@if.ufrj.br,
c.timmermans@science.ru.nl

As of early 2025, the GRAND Collaboration operates three prototype arrays: GRANDProto300 in China, GRAND@Nançay in France, and GRAND@Auger in Argentina. The GRAND@Auger prototype was established through an agreement between the GRAND and Pierre Auger Collaborations, repurposing ten Auger Engineering Radio Array (AERA) stations as GRAND detection units. This setup provides a unique opportunity for coincident air-shower detection, enabling direct event-by-event comparison between GRAND@Auger and the well-established Pierre Auger detectors. Such comparisons allow for a detailed assessment of the detection principle and reconstruction capabilities of GRAND. In this contribution, we present an overview of the commissioning and preliminary results of GRAND@Auger, including the measurement of the Galactic background noise and the detection of the first self-triggered candidate event in coincidence with the Pierre Auger Observatory. Both results underscore the role of GRAND@Auger in advancing the GRAND project and refining the techniques required for large-scale radio detection of ultra-high-energy particles.

39th International Cosmic Ray Conference (ICRC2025)
15–24 July, 2025
Geneva, Switzerland



*Speaker

1. Introduction

The Giant Radio Array for Neutrino Detection (GRAND) [1, 2] is a proposed large-scale observatory designed to identify and study the sources of ultra-high-energy cosmic rays (UHECRs). A central goal of GRAND is the detection and characterization of ultra-high-energy (UHE) neutrinos. The proposed radio-antenna array will operate by detecting radio signals produced when UHE cosmic rays, gamma rays, and neutrinos induce extensive air showers (EAS) in Earth's atmosphere. In addition, its design enables a broad range of studies in fundamental particle physics, cosmology, and radio astronomy. GRAND is expected to make significant contributions to the detection of neutrino emissions from transient astrophysical sources [3].

The GRAND Collaboration has deployed three prototype arrays: GRAND@Nançay in France [4], GRANDProto300 in China [5], and GRAND@Auger (G@A) in Argentina. These pave the way for self-triggered radio-antenna arrays capable of detecting very inclined air showers through their radio emission, a GRAND's detection concept requirement. In this paper, we focus on the G@A prototype.

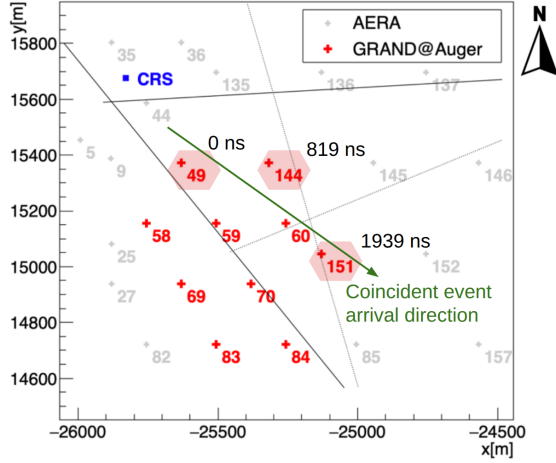


Figure 1: The layout of the G@A prototype is shown in red, with nearby AERA stations indicated in grey. The lines represent local roads. The Central Radio Station, which houses the central data acquisition computer, is highlighted in blue. The numbers in black are the timestamps in nanoseconds, relative to detection unit 49, for the coincident event that will be presented in section 4.



Figure 2: Image of one of the converted antennas at the G@A site. The 3-meter pole supports the antenna and the nut containing the LNA. Midway up the pole, the mesh communication antenna is installed. The space below the solar panel houses the battery, charge controller and front-end electronics. The entire setup is enclosed by a plastic fence.

2. The GRAND@Auger prototype

The G@A prototype represents a joint effort between the GRAND and Pierre Auger Collaborations to validate the GRAND detection concept for ultra-high-energy air showers using self-triggered radio antennas. The G@A prototype array is located at the Pierre Auger Observatory in Malargüe, Argentina, as shown in Figure 1. Ten butterfly antenna stations from the Auger Engineering Radio

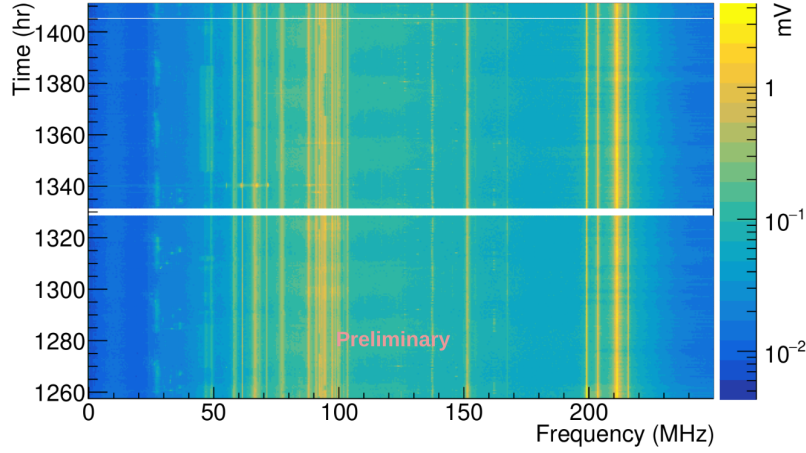


Figure 3: Periodogram of six days of data from detection unit 59. Constant radio background signals appear as vertical yellow lines, while noise-free regions are also visible. The white horizontal lines indicate hibernation periods, during which the detection unit temporarily ceased data acquisition and later resumed automatically when conditions permitted.

Array (AERA) [6] (located in the Auger’s Surface detector 750-m array) were repurposed into GRAND detection units. An array layout consisting of two superimposed hexagons with a spacing of approximately 250 m was selected. The resulting array covers an area of roughly 0.5 km². Space at the Pierre Auger Observatory’s Central Radio Station (CRS) was allocated to house the G@A Central DAQ computer. The dense layout configuration was chosen to enhance the probability of detecting lower-energy and less inclined events.

A photo of a GRAND@Auger detection unit is shown in Figure 2. Each GRAND detection unit consists of a Horizon Antenna mounted on a 3-meter pole, measuring radio signals in three polarizations: North-South (NS), East-West (EW), and Vertical (V). The mechanical structure retains some of the AERA infrastructure, including the solar panels and communication antenna, while integrating new GRAND-specific components. The Horizon Antenna is supported by a nut at the top of the pole, which also houses the low noise amplifier (LNA). Midway along the pole, the GPS and wireless communication modules are installed. At the base, a weather-sealed aluminum box contains the front-end electronics board, a battery, and a charge controller, all enclosed within Faraday cages to mitigate self-induced electromagnetic noise.

The electronic architecture includes a 500 MSPS ADC chip for digitization, combined with a Xilinx SoC processor – containing the FPGA and the CPU chips– that performs flexible filtering and triggering. The system implements a 30–200 MHz bandpass filter and applies periodic or threshold-based triggers. Data acquisition is handled locally by the on-board processor, which communicates with the central data acquisition system and sends the requested event information. These events are transmitted via a wireless TMUbiquiti Bullet-Rocket system to the central data acquisition computer at the Central Radio Station. The central system constructs the triggered events and writes them into disk, which are then transferred daily to the CCIN2P3 data center in Lyon for analysis.

GRAND Collaboration teams, aided by Pierre Auger Observatory local staff, deployed the G@A prototype array in two campaigns in March and August 2023, then followed by commissioning

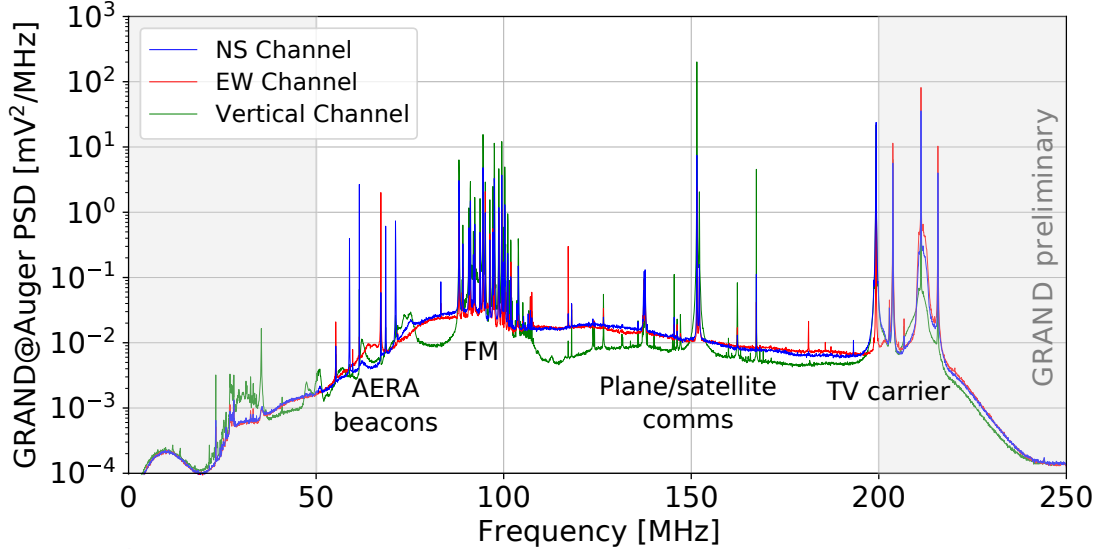


Figure 4: Average power spectral density evaluated at three polarizations over 8 hours of data from DU 83 in March 2024. The data used are from a special run of 16 μ s-long time series with a frequency resolution of approximately 62.5 kHz. Some of the known sources of the power spectrum density peaks are indicated below the PSD curves.

efforts. By March 2024, the ten G@A detection units were operational. Data taking was stable, and hibernation settings triggered by either high temperature or low battery levels were functional. An example periodogram from one detection unit, containing nearly 150 hours of continuously recorded periodically triggered data, is shown in Figure 3. Further details on the GRAND@Auger analysis and first results can be found in [7].

3. Galactic Calibration Analysis

The GRAND Collaboration makes on-going modifications and updates to the hardware and software of its prototype arrays detection units. The Galactic background analysis for the G@A prototype is based on data collected from March to June 2024, a period of stable hardware configuration. The dataset comprises measurements from the ten detection units, but careful selection and filtering were necessary to ensure data quality.

The data selection addressed the following issues:

- **Local Noise and Station-Specific Anomalies:** In some stations the electronics sporadically shows issues on gain and noise. After removal of these periods, five detection units (58, 59, 69, 144, 151) still exhibited anomalous behavior in several channels. These were excluded, leaving five detection units (49, 60, 70, 83, 84) for the Galactic analysis.
- **Single-Frequency Sources:** Narrowband radio frequency interference (e.g., video carriers, aviation communications, and satellite signals, as shown in Figure 4) was identified and removed through targeted frequency cuts, ensuring a clean broadband dataset. The filtering is done in two stages: online at the FPGA level using a programmable digital notch filter and offline at the event analysis level.

After applying all cuts, approximately 50 days of data remained for the galactic background analysis. The resulting time-averaged power spectra showed periodic features, but the limited data duration prevented a clear separation between signals following the Local Sidereal Time (LST) and those following the 24-hour GMT cycle. Longer datasets are necessary for a definitive distinction.

To interpret the measured signals, comparisons were made with simulations modeling the expected Galactic signal. The Galactic background predictions used in this analysis were produced using the LFmap program [9], which generates low-frequency sky maps for radio astronomy applications. The simulated emissions were folded with the GRAND radio frequency chain (RF chain) and were added with random Gaussian noise – implemented in the GRANDLIB software [8]. This procedure emulates the Galactic signals as if they were detected by a GRAND detection unit. A linear model was fitted to the measured power:

$$\text{Signal(LST)} = \text{Offset} + \text{Gain} \times \text{Simulation(LST)},$$

with the gain and offset optimized for each frequency range and detection unit. The analysis focused on three frequency bands: 30–200 MHz, 30–100 MHz, and 100–200 MHz. The comparison revealed:

- Better agreement at higher frequencies (100–200 MHz), where the gain calibration is understood to approximately 10% precision for horizontal polarizations and up to 50% for vertical channels.
- Weaker correlation at lower frequencies (30–100 MHz), which was also present in the full frequency range analysis (30–200 MHz). This indicates limitations in the current understanding of the system response.

The resulting data and simulation are shown in Figure 5, in which there is reasonable agreement between both. The galactic center should be turned to Malargüe at around 16-18 hours in local sidereal time (LST), then it is expected the galactic emission to have the peak amplitude. This feature can be seen in both the data and simulation. These results confirm the first detection of the Galactic background by the GRAND Collaboration at high frequencies using the G@A prototype.

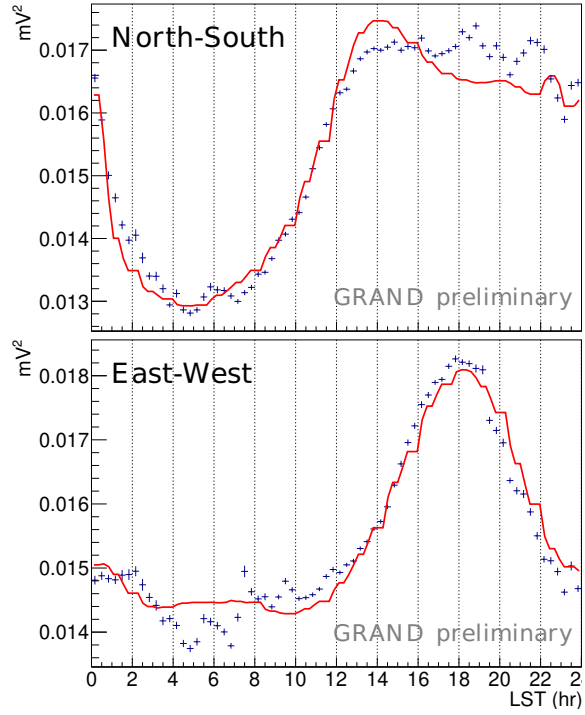


Figure 5: Data from detection unit 83 in blue, binned in 20-minute LST intervals, each line corresponds to an antenna polarization. The error bars indicate the uncertainty on the mean. The red line represents the galactic simulation fitted to the data, with an additional offset and amplification. Only the power above 100 MHz is used.

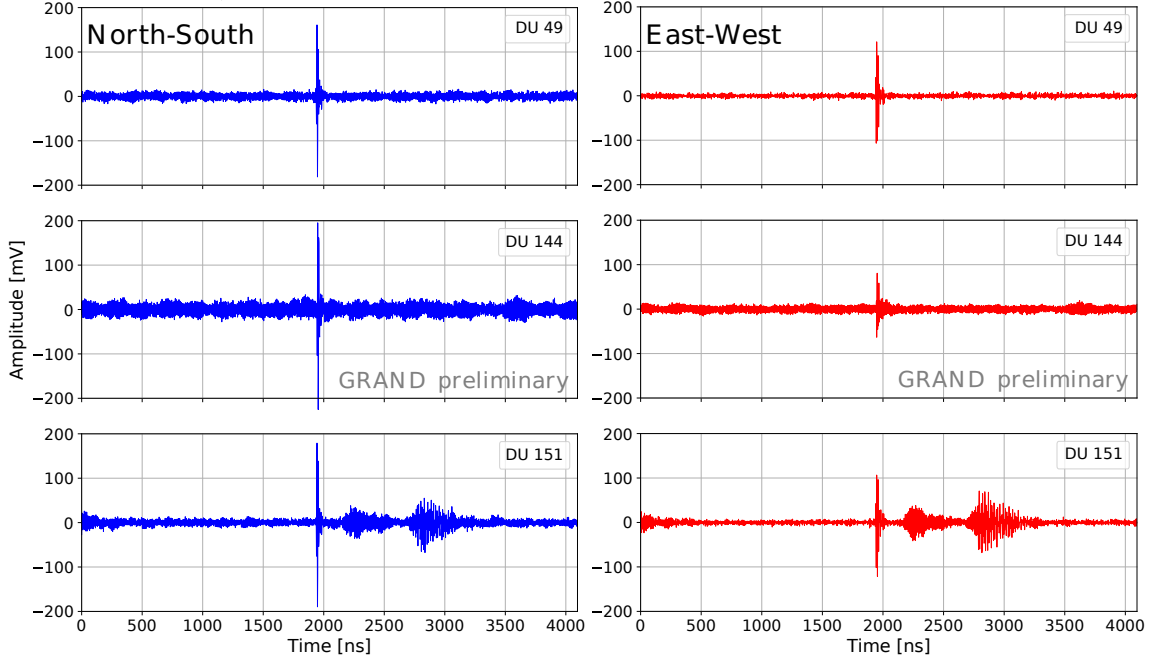


Figure 6: A self-triggered online coincidence was observed between three G@A detection units: 49, 144, and 151. The left panel shows the NS polarization for the three units, while the right panel displays the EW polarizations. A coincident signal is also present in the vertical polarization of unit 49; however, the vertical channels in units 144 and 151 were not operational.

4. G@A's First Candidate Cosmic Ray Event

The G@A prototype has identified its first candidate cosmic ray (CR) event in coincidence with a Pierre Auger Observatory triggered CR event. The G@A event occurred on September 16, 2024, at 20:06:08 UTC. It was detected as a self-triggered coincidence event across three detection units (DUs): 49, 144, and 151. The G@A timestamps for the coincident event are shown in black in Figure 1 and the raw voltage time-traces are shown in Figure 6

The G@A event, with three units in coincidence, had its arrival direction reconstructed using an analytic Plane Wave Fit [10]. The reconstruction results are as follows:

$$\phi = 143.4^\circ, \quad \theta = 77.59^\circ \quad (\text{Auger's coordinates}),$$

for ϕ the azimuth angle, measured with respect to the east, and θ the zenith angle.

The corresponding Auger event was a T5 Surface Detector (SD) event detected at the same timestamp, with 22 stations in coincidence. The Auger SD arrival direction reconstruction using a spherical wave fit yielded:

$$\phi = 142.91^\circ \pm 0.02^\circ, \quad \theta = 80.36^\circ \pm 0.05^\circ.$$

The energy estimate from the Auger SD lateral distribution function (LDF) fit was:

A time offset of approximately 10^{-6} seconds was observed between the G@A and Auger detections, with the G@A event triggering slightly earlier. The spatial and temporal coincidence, as

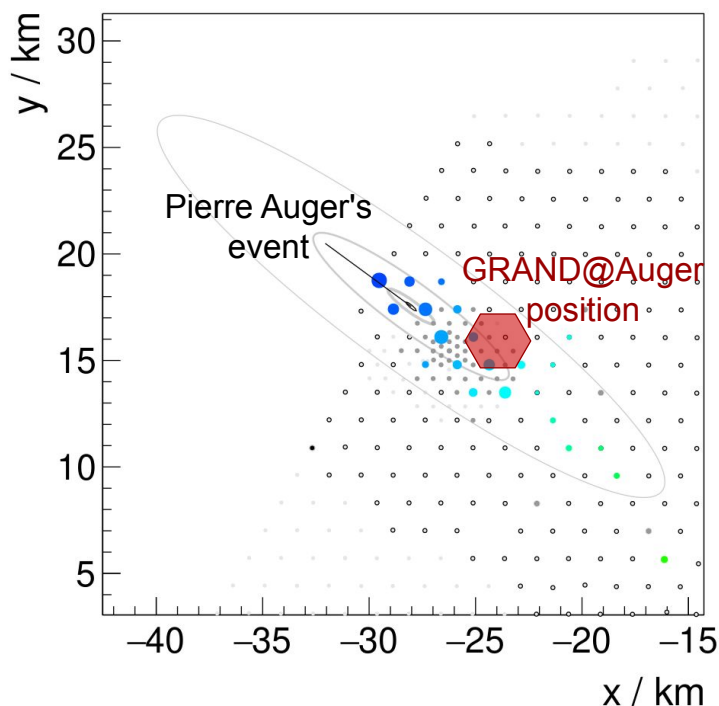


Figure 7: Coincidence event observed by the G@A prototype and the Pierre Auger Observatory on September 16, 2024, at 20:06:08 UTC. The G@A event, detected by three self-triggered GRAND units, shows a reconstructed arrival direction of $\theta = 77.6^\circ$, $\phi = 143.4^\circ$ (plane wave fit). The Auger event, detected by 22 surface stations, has a reconstructed arrival direction of $\theta = 80.4^\circ \pm 0.05^\circ$, $\phi = 142.9^\circ \pm 0.02^\circ$ (spherical wave fit) and an estimated energy of 1.39×10^{19} eV. The close match in time and direction strongly supports a common cosmic ray origin.

shown in Figure 7, along with the directional agreement from the reconstructions, provides strong evidence that this event is a cosmic ray detection by G@A. This is the first high-energy cosmic-ray event observed in coincidence by GRAND and Auger. It is also an important milestone for GRAND, which demonstrates the self-trigger capabilities of G@A and its alignment with the independent Auger reconstruction.

5. Conclusions

The G@A prototype has demonstrated stable data-taking. Self-triggered radio arrays like G@A require a precise understanding of the local electromagnetic background to optimize trigger settings and distinguish air-shower-like signals from real air-shower events. The detection of self-triggered events suggests that the trigger configuration is functioning as expected and reasonably well understood.

A detailed data cleaning procedure was implemented to identify and mitigate anthropogenic noise sources such as television signals, beacon lines, and other localized radio interference. This effort has allowed the extraction of high-quality data for further analysis.

Regarding the Galactic background, while the data set was not long enough to clearly distinguish a daily period in GMT from the expected LST periodicity without simulation support,

comparisons between the measured data and the simulations produced with LFmap show a good match, particularly at higher frequencies. In the 100–200 MHz band, the data suggest that the gain of the detector is understood to within approximately 10% for the horizontal polarizations and about 50% for the vertical channel. The G@A prototype has thus enabled the first detection of the Galactic background by GRAND at high frequencies and provided a unique measurement of the Galactic background at the Auger site in the 100–200 MHz frequency range.

Finally, the first candidate cosmic-ray event detected by G@A in coincidence with the Pierre Auger Observatory marks a significant milestone. Although the expected coincidence rate requires further investigation, the observed event, with an energy of 1.39×10^{19} eV measured by Auger, shows strong indications of being a genuine cosmic-ray event. This is the first autonomous radio detection of a cosmic ray by GRAND. The detection demonstrates the potential of the GRAND technique and highlights the importance of cross-calibration with established observatories like Pierre Auger. These results pave the way for future studies and further advances in the development of large-scale, self-triggered radio arrays for the detection of ultra-high-energy particles.

References

- [1] J. Álvarez-Muñiz *et al.* [GRAND Collaboration], “The Giant Radio Array for Neutrino Detection (GRAND): Science and Design,” *Sci. China Phys. Mech. Astron.* **63**, no.1, 219501 (2020)
- [2] O. Martineau-Huynh for the GRAND Collaboration, “The Giant Radio Array for Neutrino Detection – experimental status and plans,” *PoS ICRC2025* (2025) 1114.
- [3] C. Guépin, K. Kotera and F. Oikonomou, “High-energy neutrino transients and the future of multi-messenger astronomy,” *Nature Rev. Phys.* **4**, no.11, 697-712 (2022)
- [4] P. Correa for the GRAND Collaboration, “NUTRIG: Development of a Novel Radio Self-Trigger for GRAND,” *PoS ICRC2025* (2025) 229.
- [5] P. Ma for the GRAND Collaboration, “Progress of the GRANDProto300 Project,” *PoS ICRC2025* (2025) 453.
- [6] S. de Jong for the Pierre Auger Collaboration, “Detection of High Energy Cosmic Rays at the Auger Engineering Radio Array,” *PoS ICHEP2016* (2017) 080.
- [7] B. de Errico for the GRAND Collaboration, “GRAND@Auger: status and first results,” *PoS UHECR2024* (2024) 076.
- [8] R. Alves Batista *et al.* [GRAND Collaboration], *GRANDlib: A simulation pipeline for the Giant Radio Array for Neutrino Detection (GRAND)*, *Computer Physics Communications*, vol. 308, 2025, 109461.
- [9] E. Polisensky, “LFmap: A Low Frequency Sky Map Generating Program”, *Long Wavelength Array (LWA) Memo Series*, 111 (2007).
- [10] A. Ferrière *et al.*, “Analytical planar wavefront reconstruction and error estimates for radio detection of extensive air showers”, *arXiv:2408.15677* (2024).

Full Author List: GRAND Collaboration

J. Álvarez-Muñiz¹, R. Alves Batista^{2,3}, A. Benoit-Lévy⁴, T. Bister^{5,6}, M. Bohacova⁷, M. Bustamante⁸, W. Carvalho⁹, Y. Chen^{10,11}, L. Cheng¹², S. Chiche¹³, J. M. Colley³, P. Correa³, N. Cucu Laurenciu^{5,6}, Z. Dai¹¹, R. M. de Almeida¹⁴, B. de Errico¹⁴, J. R. T. de Mello Neto¹⁴, K. D. de Vries¹⁵, V. Decoene¹⁶, P. B. Denton¹⁷, B. Duan^{10,11}, K. Duan¹⁰, R. Engel^{18,19}, W. Erba^{20,21}, Y. Fan¹⁰, A. Ferrière^{4,3}, Q. Gou²², J. Gu¹², M. Guelfand^{3,2}, G. Guo²³, J. Guo¹⁰, Y. Guo²², C. Guépin²⁴, L. Güllow¹⁸, A. Haungs¹⁸, M. Havelka⁷, H. He¹⁰, E. Hivon², H. Hu²², G. Huang²³, X. Huang¹⁰, Y. Huang¹², T. Huege^{25,18}, W. Jiang²⁶, S. Kato², R. Koirala^{27,28,29}, K. Kotera^{2,15}, J. Köhler¹⁸, B. L. Lago³⁰, Z. Lai³¹, J. Lavoisier^{2,20}, F. Legrand³, A. Leisos³², R. Li²⁶, X. Li²², C. Liu²², R. Liu^{28,29}, W. Liu²², P. Ma¹⁰, O. Macías^{31,33}, F. Magnard², A. Marcowith²⁴, O. Martineau-Huynh^{3,12,2}, Z. Mason³¹, T. McKinley³¹, P. Minodier^{20,2,21}, M. Mostafa³⁴, K. Murase^{35,36}, V. Niess³⁷, S. Nonis³², S. Ogio^{21,20}, F. Oikonomou³⁸, H. Pan²⁶, K. Papageorgiou³⁹, T. Pierog¹⁸, L. W. Piotrowski⁹, S. Pruner⁴⁰, C. Prévotat², X. Qian⁴¹, M. Roth¹⁸, T. Sako^{21,20}, S. Shinde³¹, D. Szálas-Motesiczky^{5,6}, S. Ślawiński⁹, K. Takahashi²¹, X. Tian⁴², C. Timmermans^{5,6}, P. Tobiska⁷, A. Tsirigotis³², M. Tüeros⁴³, G. Vittakis³⁹, V. Voisin³, H. Wang²⁶, J. Wang²⁶, S. Wang¹⁰, X. Wang^{28,29}, X. Wang⁴¹, D. Wei¹⁰, F. Wei²⁶, E. Weissling³¹, J. Wu²³, X. Wu^{12,44}, X. Wu⁴⁵, X. Xu²⁶, X. Xu^{10,11}, F. Yang²⁶, L. Yang⁴⁶, X. Yang⁴⁵, Q. Yuan¹⁰, P. Zarka⁴⁷, H. Zeng¹⁰, C. Zhang^{42,48,28,29}, J. Zhang¹², K. Zhang^{10,11}, P. Zhang²⁶, Q. Zhang²⁶, S. Zhang⁴⁵, Y. Zhang¹⁰, H. Zhou⁴⁹

¹Departamento de Física de Partículas & Instituto Galego de Física de Altas Enerxías, Universidad de Santiago de Compostela, 15782 Santiago de Compostela, Spain

²Institut d'Astrophysique de Paris, CNRS UMR 7095, Sorbonne Université, 98 bis bd Arago 75014, Paris, France

³Sorbonne Université, Université Paris Diderot, Sorbonne Paris Cité, CNRS, Laboratoire de Physique Nucléaire et de Hautes Energies (LPNHE), 4 Place Jussieu, F-75252, Paris Cedex 5, France

⁴Université Paris-Saclay, CEA, List, F-91120 Palaiseau, France

⁵Institute for Mathematics, Astrophysics and Particle Physics, Radboud Universiteit, Nijmegen, the Netherlands

⁶Nikhef, National Institute for Subatomic Physics, Amsterdam, the Netherlands

⁷Institute of Physics of the Czech Academy of Sciences, Na Slovance 1999/2, 182 00 Prague 8, Czechia

⁸Niels Bohr International Academy, Niels Bohr Institute, University of Copenhagen, 2100 Copenhagen, Denmark

⁹Faculty of Physics, University of Warsaw, Pasteura 5, 02-093 Warsaw, Poland

¹⁰Key Laboratory of Dark Matter and Space Astronomy, Purple Mountain Observatory, Chinese Academy of Sciences, 210023 Nanjing, Jiangsu, China

¹¹School of Astronomy and Space Science, University of Science and Technology of China, 230026 Hefei Anhui, China

¹²National Astronomical Observatories, Chinese Academy of Sciences, Beijing 100101, China

¹³Inter-University Institute For High Energies (IIHE), Université libre de Bruxelles (ULB), Boulevard du Triomphe 2, 1050 Brussels, Belgium

¹⁴Instituto de Física, Universidade Federal do Rio de Janeiro, Cidade Universitária, 21.941-611- Ilha do Fundão, Rio de Janeiro - RJ, Brazil

¹⁵IIHE/ELEM, Vrije Universiteit Brussel, Pleinlaan 2, 1050 Brussels, Belgium

¹⁶SUBATECH, Institut Mines-Telecom Atlantique, CNRS/IN2P3, Université de Nantes, Nantes, France

¹⁷High Energy Theory Group, Physics Department Brookhaven National Laboratory, Upton, NY 11973, USA

¹⁸Institute for Astroparticle Physics, Karlsruhe Institute of Technology, D-76021 Karlsruhe, Germany

¹⁹Institute of Experimental Particle Physics, Karlsruhe Institute of Technology, D-76021 Karlsruhe, Germany

²⁰ILANCE, CNRS – University of Tokyo International Research Laboratory, Kashiwa, Chiba 277-8582, Japan

²¹Institute for Cosmic Ray Research, University of Tokyo, 5 Chome-1-5 Kashiwanoha, Kashiwa, Chiba 277-8582, Japan

²²Institute of High Energy Physics, Chinese Academy of Sciences, 19B YuquanLu, Beijing 100049, China

²³School of Physics and Mathematics, China University of Geosciences, No. 388 Lumo Road, Wuhan, China

²⁴Laboratoire Univers et Particules de Montpellier, Université Montpellier, CNRS/IN2P3, CC72, Place Eugène Bataillon, 34095, Montpellier Cedex 5, France

²⁵Astrophysical Institute, Vrije Universiteit Brussel, Pleinlaan 2, 1050 Brussels, Belgium

²⁶National Key Laboratory of Radar Detection and Sensing, School of Electronic Engineering, Xidian University, Xi'an 710071, China

²⁷Space Research Centre, Faculty of Technology, Nepal Academy of Science and Technology, Khumaltar, Lalitpur, Nepal

²⁸School of Astronomy and Space Science, Nanjing University, Xianlin Road 163, Nanjing 210023, China

²⁹Key laboratory of Modern Astronomy and Astrophysics, Nanjing University, Ministry of Education, Nanjing 210023, China

³⁰Centro Federal de Educação Tecnológica Celso Suckow da Fonseca, UnED Petrópolis, Petrópolis, RJ, 25620-003, Brazil

³¹Department of Physics and Astronomy, San Francisco State University, San Francisco, CA 94132, USA

³²Hellenic Open University, 18 Aristotelous St, 26335, Patras, Greece

³³GRAPPA Institute, University of Amsterdam, 1098 XH Amsterdam, the Netherlands

³⁴Department of Physics, Temple University, Philadelphia, Pennsylvania, USA

³⁵Department of Astronomy & Astrophysics, Pennsylvania State University, University Park, PA 16802, USA

³⁶Center for Multimessenger Astrophysics, Pennsylvania State University, University Park, PA 16802, USA

³⁷CNRS/IN2P3 LPC, Université Clermont Auvergne, F-63000 Clermont-Ferrand, France

³⁸Institutt for fysikk, Norwegian University of Science and Technology, Trondheim, Norway

³⁹Department of Financial and Management Engineering, School of Engineering, University of the Aegean, 41 Kountouriotou Chios,

Northern Aegean 821 32, Greece

⁴⁰Laboratoire Lagrange, Observatoire de la Côte d’Azur, Université Côte d’Azur, CNRS, Parc Valrose 06104, Nice Cedex 2, France

⁴¹Department of Mechanical and Electrical Engineering, Shandong Management University, Jinan 250357, China

⁴²Department of Astronomy, School of Physics, Peking University, Beijing 100871, China

⁴³Instituto de Física La Plata, CONICET - UNLP, Boulevard 120 y 63 (1900), La Plata - Buenos Aires, Argentina

⁴⁴Shanghai Astronomical Observatory, Chinese Academy of Sciences, 80 Nandan Road, Shanghai 200030, China

⁴⁵Purple Mountain Observatory, Chinese Academy of Sciences, Nanjing 210023, China

⁴⁶School of Physics and Astronomy, Sun Yat-sen University, Zhuhai 519082, China

⁴⁷LIRA, Observatoire de Paris, CNRS, Université PSL, Sorbonne Université, Université Paris Cité, CY Cergy Paris Université, 92190 Meudon, France

⁴⁸Kavli Institute for Astronomy and Astrophysics, Peking University, Beijing 100871, China

⁴⁹Tsung-Dao Lee Institute & School of Physics and Astronomy, Shanghai Jiao Tong University, 200240 Shanghai, China

Acknowledgments

The GRAND Collaboration is grateful to the local government of Dunhuang during site survey and deployment approval, to Tang Yu for his help on-site at the GRANDProto300 site, and to the Pierre Auger Collaboration, in particular, to the staff in Malargüe, for the warm welcome and continuing support. The GRAND Collaboration acknowledges the support from the following funding agencies and grants. **Brazil:** Conselho Nacional de Desenvolvimento Científico e Tecnológico (CNPq); Fundação de Amparo à Pesquisa do Estado de Rio de Janeiro (FAPERJ); Coordenação Aperfeiçoamento de Pessoal de Nível Superior (CAPES). **China:** National Natural Science Foundation (grant no. 12273114); NAOC, National SKA Program of China (grant no. 2020SKA0110200); Project for Young Scientists in Basic Research of Chinese Academy of Sciences (no. YSBR-061); Program for Innovative Talents and Entrepreneurs in Jiangsu, and High-end Foreign Expert Introduction Program in China (no. G2023061006L); China Scholarship Council (no. 202306010363); and special funding from Purple Mountain Observatory. **Denmark:** Villum Fonden (project no. 29388). **France:** “Emergences” Programme of Sorbonne Université; France-China Particle Physics Laboratory; Programme National des Hautes Energies of INSU; for IAP—Agence Nationale de la Recherche (“APACHE” ANR-16-CE31-0001, “NUTRIG” ANR-21-CE31-0025, ANR-23-CPJ1-0103-01), CNRS Programme IEA Argentine (“ASTRONU”, 303475), CNRS Programme Blanc MITI (“GRAND” 2023.1 268448), CNRS Programme AMORCE (“GRAND” 258540); Fulbright-France Programme; IAP+LPNHE—Programme National des Hautes Energies of CNRS/INSU with INP and IN2P3, co-funded by CEA and CNES; IAP+LPNHE+KIT—NuTRIG project, Agence Nationale de la Recherche (ANR-21-CE31-0025); IAP+VUB: PHC TOURNESOL programme 48705Z. **Germany:** NuTRIG project, Deutsche Forschungsgemeinschaft (DFG, Projektnummer 490843803); Helmholtz—OCPC Postdoc-Program. **Poland:** Polish National Agency for Academic Exchange within Polish Returns Program no. PPN/PPO/2020/1/00024/U/00001,174; National Science Centre Poland for NCN OPUS grant no. 2022/45/B/ST2/0288. **USA:** U.S. National Science Foundation under Grant No. 2418730. Computer simulations were performed using computing resources at the CCIN2P3 Computing Centre (Lyon/Villeurbanne, France), partnership between CNRS/IN2P3 and CEA/DSM/Irfu, and computing resources supported by the Chinese Academy of Sciences.